IRANIAN JOURNAL OF CATALYSIS

IJC
Iranian Journal of Catalysis

Sol-gel synthesis of nanoporous γ-alumina using TX-100 or gelatin/TX-100 mixture as effective catalysts for dehydration of alcohols

Soheyl Alidoust, Mehdi Zamani*, Morteza Jabbari

School of Chemistry, Damghan University, Damghan 36716-41167, Iran

ABSTRACT

In this study, the nanoporous γ-alumina catalysts were prepared by the sol-gel method using hydrolysis of aluminum isopropoxide in the presence of TX-100 or gelatin/TX-100 mixture. Catalysts were characterized by XRD, FT-IR, TEM, BET-BJH and N_2 adsorption-desorption isotherms. To investigate reactivity and selectivity of the synthesized catalysts, dehydration reaction of 2-octanol was carried out in a plug flow vertical reactor at 200 °C. The main products of elimination reaction were 1-octene, 3-octene, *cis*- and *trans*-2-octene, which were identified by GC-MS. The reaction conversion and yield of the products were determined using GC. The prepared catalysts had nanometer-sized pores, high surface area and large pore volume. Their catalytic activity for dehydration of 2-octanol was higher than non-porous γ-alumina catalysts. These compounds could be used as effective catalysts for dehydration of alcohols.

Keywords: *γ-Alumina, Nanoporous, Triton X-100, Gelatin, Dehydration, Alcohol, Alkene.*

1. Introduction

Alumina is an amphoteric oxide of aluminum with the chemical formula of Al_2O_3. Corundum is the most common naturally occurring crystalline form of alumina which typically contains traces of iron, titanium, vanadium and chromium [1]. Alumina is a set of structural polymorphs that include α-alumina and various metastable types (χ, κ, γ, δ, θ and η) [2]. This compound is produced by the Bayer process from bauxite [3]. Bauxite is made up of a mixture of aluminum hydroxide materials including gibbsite [Al(OH)$_3$], boehmite [AlO(OH)] and diaspore [α-AlO(OH)] [3]. Zamani and coworkers studied the effects of vacuum and calcination temperature on the structure and texture of alumina [4]. They found that heating of boehmite to above 450 °C leads to the formation of γ-alumina [4]. While it was reported that the formation of α-alumina occurs at temperatures as high as 1200 °C [5]. The major uses of alumina materials are in refractories, ceramics, abrasives, drying agents, adsorbents, fillers and catalysts [6]. The catalytic performance of alumina materials is largely dependent on the type of alumina phase and textural properties.

*Corresponding author:
E-mail address: m.zamani@du.ac.ir. (M. Zamani)

Alumina materials with large surface area, large pore volume, narrow pore size distribution and suitable surface acidic-basic properties can often result in favorable enhancement in the catalytic performance [7]. γ-Alumina is an important catalyst in academic researches and industries, because it has a large surface area and high capacity for absorption of various molecules [8]. Adsorption and reactions of alcohols over γ-alumina plays an increasingly important role in modern surface science and technology. Zamani and Dabbagh reported the adsorption of a variety of primary, secondary and tertiary alcohols with alkyl, allyl and aryl substituents (i.e. methanol, ethanol, 1-propanol, 2-propanol, 1-butanol, 2-butanol, *t*-butanol, 2-octanol, cyclohexanol, allyl alcohol, benzyl alcohol, phenol, etc.) over γ-alumina surface [9]. The adsorption and reaction mechanisms for ethanol dehydration and etherification on γ-alumina were studied by Christiansen et al. [10] and Fang et al. [11]. The alkene/ether selectivity for dehydration reaction of isopropanol over γ-alumina was studied by Larmier et al. [12]. Methanol and dimethyl ether adsorption and the formation mechanism of dimethyl ether from methanol dehydration over γ-alumina were studied by Zuo et al. [13, 14]. The mechanism of adsorption, dissociation, hydrogen-shift, dehydration and dehydrogenation of 2-

butanol over γ-alumina were investigated by Zamani and coworkers [15].

The synthesis of porous alumina materials has attracted much attention in recent years. For instance, Chen et al. reported the synthesis of uniform mesoporous alumina with excellent thermal stability and controllable pore size distribution through ultrasonic assisted sol-gel method [16]. Song et al. reported the synthesis of mesoporous alumina nanofibers using polyvinyl butyral (PVB) as polymer template via electrospinning technique [17]. Hu et al. reported the synthesis, characterization and application of mesoporous alumina prepared from pseudo-boehmite as precursor and selected group of surfactants including sodium dodecylsulphate (SDS), cetyltrimethylammonium bromide (CTAB) and polyethylene glycol (PEG) [18]. Ambade et al. reported the synthesis of mesoporous alumina by mechanochemical approach [19]. Chakravarty et al. reported the synthesis of high surface area mesoporous alumina with narrow pore size distribution by solid state reaction [20]. Derakhshani et al. reported the synthesis of mesoporous γ-alumina with high degree of crystallinity, large surface area and pore volume using carbonization of metal-organic framework derived nanoporous carbon template [21]. Liu et al. reported the synthesis of spongy mesoporous γ-alumina using Al-based metal-organic frameworks as precursor by two-step pyrolysis [22]. Compared with industrial γ-alumina, the spongy alumina displayed well-developed porosity with relatively high surface area, large pore volume, and abundant weak Lewis acid sites [22]. Mohammadnezhad et al. reported the sol-gel synthesis of highly thermally stable nanoporous alumina materials using various alkoxide precursors and Pluronic P123 copolymer template [23]. For the prepared compounds, excellent thermal stability and adjustable pore size distribution were found [23]. Berger et al. reported the synthesis of mesoporous alumina from aluminum isopropoxide in the presence of fatty acids (e.g. lauric and stearic acid), CTAB and P123 templates [24]. The obtained compounds have high specific surface area, narrow pore size distribution, and different morphology depending on the template used in the synthesis [24].

Triton X-100 (TX-100) is a nonionic surfactant which has a hydrophilic polyethylene oxide head and a hydrocarbon hydrophobic tail [25]. This compound was used for the synthesis of hierarchically organized urchin-like hollow boehmite and alumina microspheres with large surface area and pore volume using aluminum sulfate and urea through the hydrothermal route [26]. Gelatin is an important biomolecule derived from collagen which is commonly used as a gelling agent [27]. This compound was used as template for the synthesis of low surface area amorphous and γ-alumina containing micro/mesopores using aluminum nitrate through the sol-gel method [28, 29].

In the present study, we report the sol-gel synthesis of nanoporous γ-alumina using hydrolysis of aluminum isopropoxide in the presence of TX-100 (as surfactant) or TX-100 in aqueous solution of gelatin (as template). The morphology of catalysts was studied by X-ray diffraction (XRD), Fourier-transform infrared (FT-IR) spectroscopy and transmission electron microscopy (TEM). The Brunauer-Emmett-Teller (BET) and Barrett-Joyner-Halenda (BJH) measurements as well as N_2 adsorption-desorption isotherms were used for determination of specific surface areas, pore volumes, mean pore diameters, pore size distributions and the cavity shapes. It is well known that γ-alumina is an excellent catalyst for dehydration of alcohols to alkenes [30, 31] to evaluate the catalytic activity and selectivity of catalysts, the dehydration reaction of 2-octanol was carried out at 200 °C. The results were also compared with the literature data.

2. Experimental

2. 1. Materials and instruments

The chemicals used in this study, including aluminum isopropoxide (Al(O-i-Pr)$_3$), isopropanol (i-PrOH), Triton X-100 (TX-100) and 2-octanol were purchased from Merck Chemical Co; and pure gelatin powder was prepared from the Farmand factory, Iran. Materials were weighed on an analytical balance Kern, ACJ 220-4M model. The XRD measurements were carried out using Bruker D8-Advance diffractometer with CuKα radiation in the range between 2θ = 10-80°. The FT-IR spectra were recorded using KBr pellets on Perkin-Elmer RXI Fourier transform infrared spectrophotometer in the wave number range from 400 to 3500 cm^{-1}. To measure the specific surface areas, pore volumes, N_2 adsorption-desorption isotherms, BET and BJH measurements, the BEL BELSORP MINI II device was used. The TEM pictures were taken by Leo 912 AB transmission electron microscope. The elimination reactions of 2-octanol were performed using in-home plug flow vertical reactor apparatus. The SP1000HOM digital injection pump manufactured by Iran Nanoscale Technologies Co. with a timing and flow rate control system was used for pumping 2-octanol over the catalysts. Analysis of the products mixture for dehydration of 2-octanol was carried out by gas chromatography mass spectrometry (GC-MS) Fisons 8060 instrument (QD analyzer and Trio 1000 detector model) equipped with a 30 m HP-5 capillary column. The Varian CP3800 gas chromatography (GC)

apparatus equipped with a flame ionization detector (FID) was used for the determination of reaction conversion and yield of the products. The GC analysis was performed using 30 m CP-Sil 5 CB capillary column at a constant carrier gas (argon) flow rate of 2 mL/min. Samples were injected using the split mode at 50:1. The injector and detector temperatures were held at 200 and 250 °C, respectively. The products were separated using the following oven program: 2 min at 45 °C, first ramp at 10 °C/min to 75 °C (held for 12 min), second ramp at 20 °C/min to 140 °C (held for 2 min).

2.2. Catalysts preparation

The nanoporous γ-alumina catalysts were synthesized with two different protocols using sol-gel method. The first catalyst was prepared by hydrolysis of aluminum isopropoxide in the presence of non-ionic surfactant TX-100. For this purpose, aluminum isopropoxide (10 g) and isopropanol (10 mL) were mixed and stirred for 30 min at room temperature. Then, the mixture of TX-100 (5 mL) and isopropanol (5 mL) was added to this mixture, and the solution was stirred for another 1 h at room temperature. Then, deionized water (30 mL) was added gradually to the reaction vessel with continuous stirring for 4.5 h, until a milky gel was formed. The resulting gel was kept at room temperature for 12 h under static condition to perform the ageing process. Then, the sample was heated in an oven at 110 °C for 12 h to complete drying. The powder was then calcined at 600 °C for 6 h in a furnace to remove the surfactant and for the formation of the porous catalyst.

The second catalyst was prepared by hydrolysis of aluminum isopropoxide in the presence of gelatin/TX-100 mixture. TX-100 and gelatin were chosen as the surfactant and template, respectively. For this purpose, aluminum isopropoxide (10 g) and isopropanol (10 mL) were mixed and stirred for 30 min at room temperature. After the mixture of TX-100 (5 mL) and isopropanol (5 mL) was added, the solution was stirred for 1 h at room temperature. Then, gelatin (2 g) was dissolved in deionized water (30 mL) at 50 °C, and the solution was added gradually to the reaction vessel with continuous stirring for 4.5 h. During this time, a milky gel was formed. After ageing at room temperature for 12 h, the gel was dried at 110 °C for 12 h. The porous catalyst was obtained from dried gel after being calcined at 600 °C for 6 h to remove the template/surfactant.

2.3. Dehydration reaction

The conversion of 2-octanol over nanoporous γ-alumina catalysts was performed, according to our previous published articles [4, 30, 31] in a plug flow vertical reactor made of Pyrex glass and fitted with a thermal well that extended to the center of the catalyst bed. Initially, the catalyst was activated in air at 300 °C for 2 h. Then, 2-octanol was injected with flow rate 5 mL/h over 0.5 g catalyst at 200 °C (reaction temperature). The liquid products were collected after passing through a water-cooled condenser (with increasing time intervals).

3. Results and Discussion

The nanoporous γ-alumina catalysts are prepared by sol-gel method using hydrolysis of aluminum isopropoxide in the presence of TX-100 or gelatin/TX-100 mixture. The precursor solution is made of aluminum isopropoxide dissolved in isopropanol as solvent. The non-ionic surfactant TX-100 is mixed with isopropanol as co-surfactant. Gelatin is used as a template and gelling agent (**Scheme 1**).
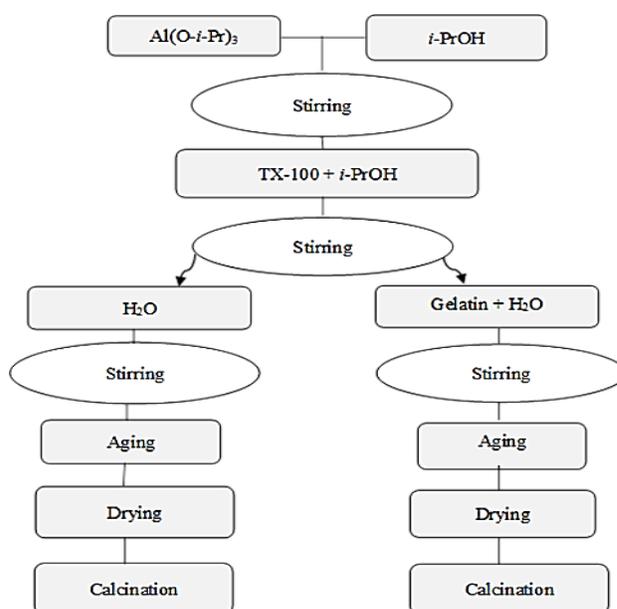
Scheme 1. Two protocols used for the synthesis of nanoporous γ-alumina catalysts in this study.

The XRD patterns of the synthesized catalysts in comparison to commercial nano γ-alumina are shown in **Fig. 1**. Both catalysts display a similar pattern attributed to alumina γ-phase, where characteristic diffraction peaks at 38, 46 and 67° are assigned to the (311), (400) and (440) planes of γ-alumina, respectively [2]. The broadening of XRD pattern at about 30-40° for the synthesized catalysts in comparison to commercial γ-alumina corresponds to the formation of amorphous alumina in small amounts. Also, the degree of crystallinity for nanoporous catalysts is slightly lower than commercial nano γ-alumina. The crystallite sizes inferred from the width of (400) and (440) peaks through the Scherrer equation for commercial nano γ-alumina are 4.2 and 5.2 nm, respectively. The corresponding values for nanoporous

γ-alumina prepared using TX-100 are 11.0 and 10.1, respectively. These values are larger than the crystallite sizes investigated for catalyst synthesized using gelatin/TX-100 mixture 6.8 and 6.1 nm, respectively.
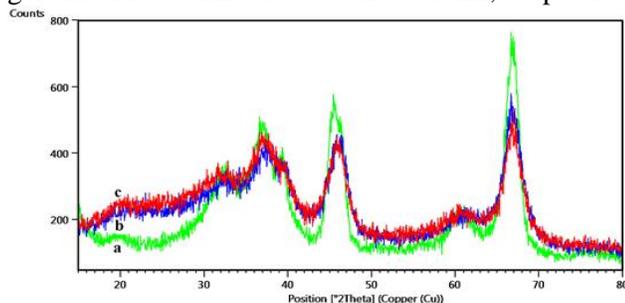

Fig. 1. XRD patterns for the synthesized nanoporous γ-alumina catalysts using TX-100 (b) and gelatin/TX-100 (c) in comparison to commercial γ-alumina (a).

The FT-IR spectra of synthesized nanoporous catalysts in comparison to commercial γ-alumina are shown in **Fig. 2**. The FT-IR spectrum of commercial γ-alumina shows five absorption bands at 552, 755, 1384, 1635 and 3476 cm^{-1}. The peaks appearing at 552 and 755 cm^{-1} are assigned to ν-AlO$_4$ and ν-AlO$_6$ corresponding to the tetrahedral and octahedral aluminum atoms [4]. The observed peaks at 1384 and 1635 are related to the bending vibrations of surface hydroxyl groups (Al–OH) and adsorbed water on the surface (Al–OH$_2$) [8]. The peak displayed at 3476 cm^{-1} is attributed to O–H stretching mode. The prepared catalyst using TX-100 surfactant exhibits absorption bands at 898, 1408, 1638 and 3472 cm^{-1}. The prepared catalyst using gelatin/TX-100 mixture shows the vibration mods at 1108, 1404, 1638 and 3452 cm^{-1}. The peak merged at 1108 cm^{-1} is assigned to Al–O–Al bending vibrations [32]. Formation of Al–O–Al bond might be a consequence of the condensation of Al–OH groups located on the outer surface of alumina and the formation of porous structure.

The BET-BJH measurements, nitrogen adsorption-desorption isotherms and TEM images were used for studying the textual structure of nanoporous catalysts. **Fig. 3** shows the BET curves for the synthesized compounds. The total BET surface areas for the γ-alumina synthesized through hydrolysis of aluminum isopropoxide in the presence of gelatin/TX-100 and TX-100 are 275.0 and 289.4 m^2 g^{-1}, respectively. Both of these values are higher than the specific surface area reported for commercial nano γ-alumina (i.e. 138 m^2 g^{-1}) [8] and γ-alumina prepared under hydrolysis of aluminum isopropoxide without using surfactant and/or template (i.e. 150 m^2 g^{-1}) [4, 30, 31].

The BJH pore size distributions for the synthesized catalysts are shown in **Fig. 4**.
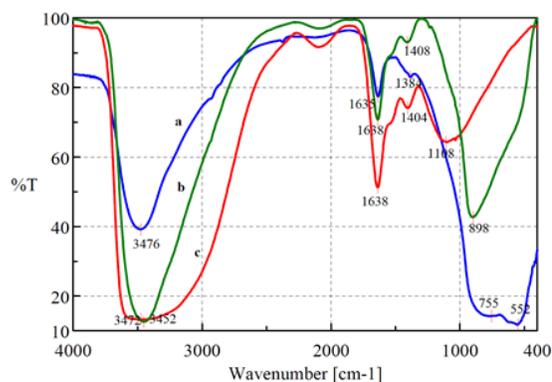

Fig. 2. FT-IR spectra for the synthesized nanoporous γ-alumina catalysts using TX-100 (a) and gelatin/TX-100 (b).
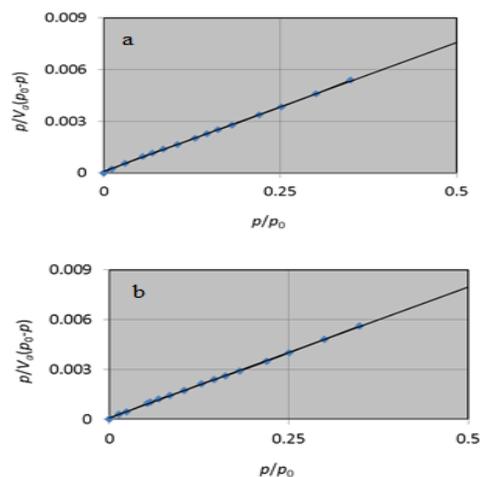

Fig. 3. BET curves for the synthesized nanoporous γ-alumina catalysts using TX-100 (a) and gelatin/TX-100 (b).

The pore size distribution curves fall into the 2–50 nm range, which is the characteristic for mesopores. Both compounds show relatively wide pore size distributions with a centered peak at 7 and 10 nm for the prepared catalysts using gelatin/TX-100 and TX-100, respectively. The prepared catalysts using gelatin/TX-100 and TX-100 have the total pore volumes of 1.07 and 1.62 cm^3 g^{-1}, and the average pore diameters of 15.56 and 22.44 nm, respectively. A number of porous alumina compounds reported in the literatures which had lower [23, 28, 33, 34] or higher [22] surface areas and/or pore volumes than those reported in this study. According to the results, the nanoporous γ-alumina prepared using TX-100 has larger surface area, pore volume and average pore diameter than the nanoporous catalyst prepared using gelatin/TX-100. Therefore, the effect of TX-100 on the textural structure of porous γ-alumina is more significant.

The N$_2$ adsorption-desorption isotherms for nanoporous catalysts are presented in **Fig. 5**. Both catalysts display type IV isotherms based on the classification of sorption isotherms [35].
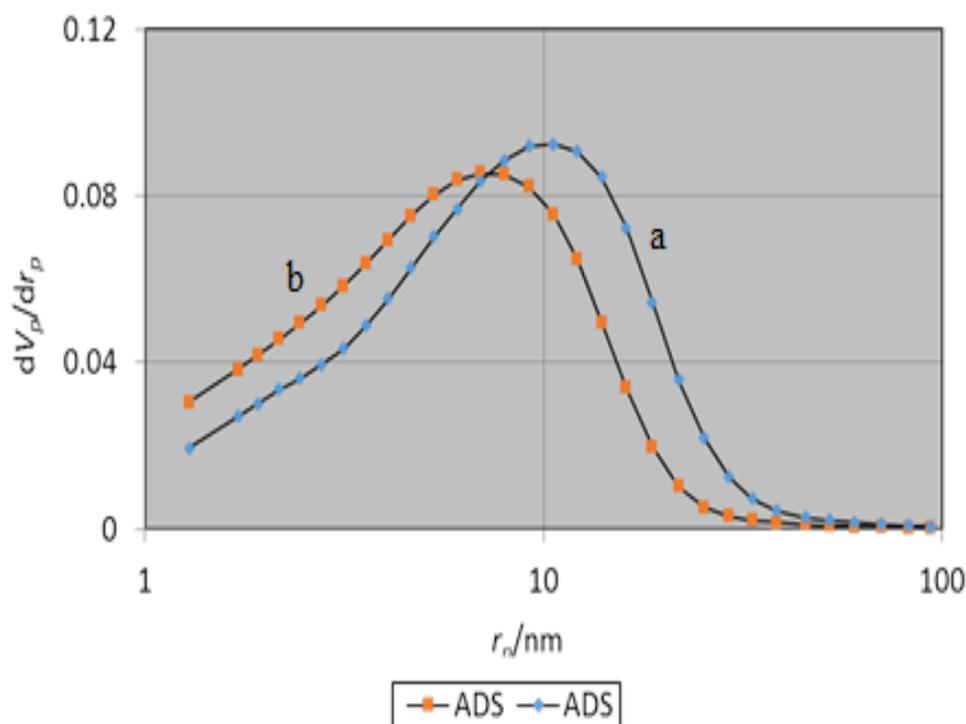
Fig. 4. BJH pore size distribution curves for the synthesized nanoporous γ-alumina catalysts using TX-100 (a) and gelatin/TX-100 (b).

The characteristic feature of this type of isotherm is narrow hysteresis loop between the adsorption and desorption diagrams at high relative pressures [36]. This type of isotherm is typical for mesoporous materials with cylindrical shape pores. TEM images for the synthesized catalysts are shown in **Fig. 6**, which reveal porous texture of the catalysts.
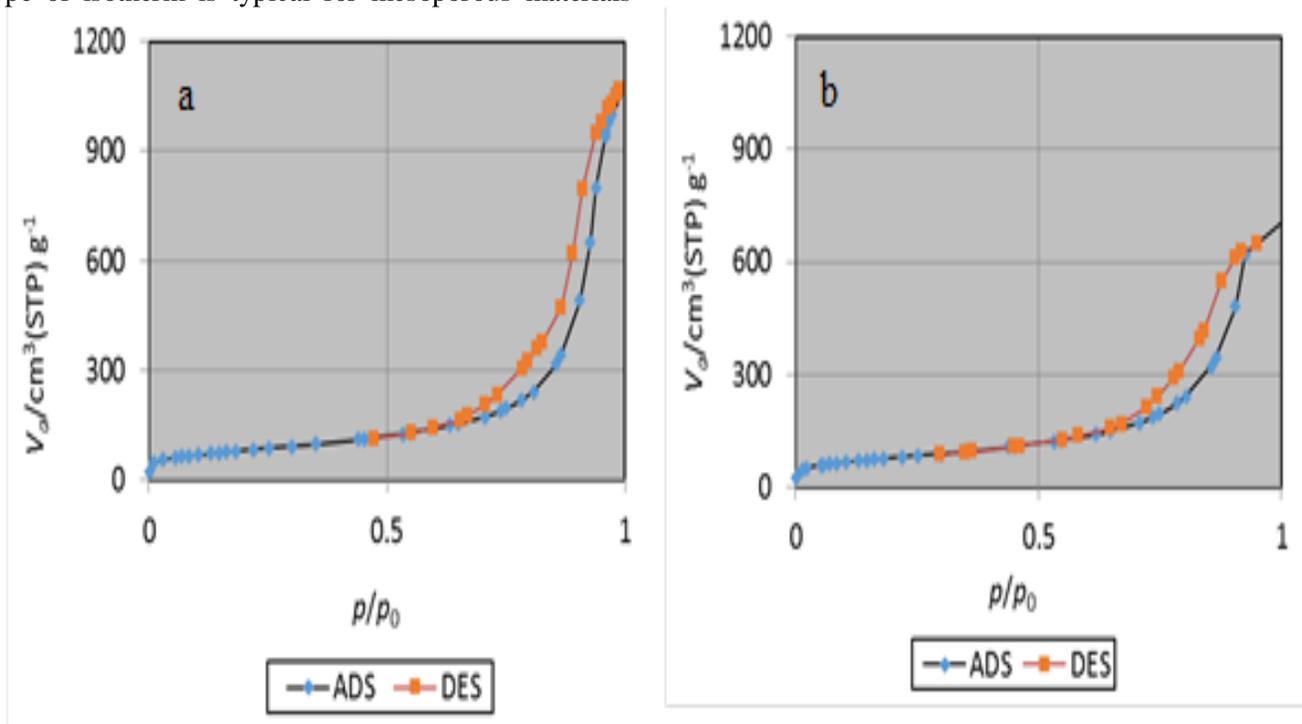

Fig. 5. The N_2 adsorption-desorption isotherms for the synthesized nanoporous γ-alumina catalysts using TX-100 (a) and gelatin/TX-100 (b).
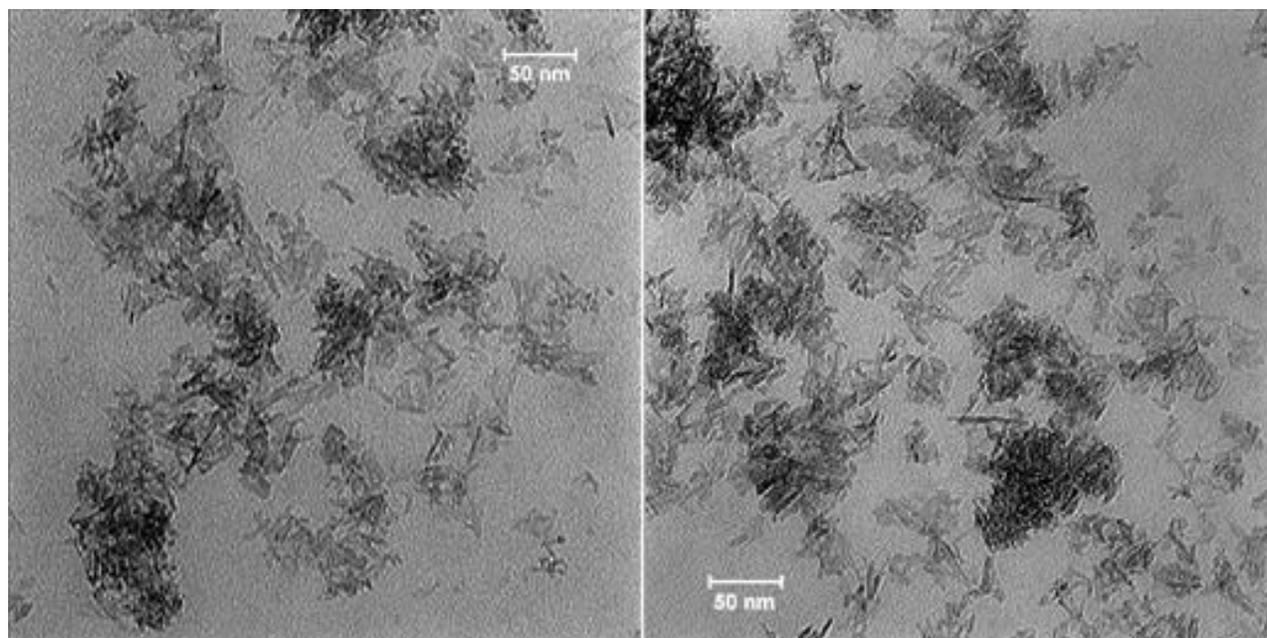
Fig. 6. TEM images for the synthesized nanoporous γ-alumina catalysts using TX-100 (right) and gelatin/TX-100 (left).

To investigate the reactivity and selectivity of the synthesized catalysts, the dehydration reaction of 2-octanol was carried out in a plug flow vertical reactor at 200 °C. The conversion percentage and yield of the main products for elimination reaction of 2-octanol over the synthesized catalysts are listed in **Tables 1** and **2**. The main products of the elimination reaction are 1-octene, 3-octene, *cis-* and *trans-*2-octene. The average conversion percentage for the prepared nanoporous γ-alumina using gelatin/TX-100 is 93.10%. The corresponding value for the prepared catalyst using TX-100 is 99.58%. The average percentage of products yield for the former catalyst are *cis-*2-octene (36.39%), 1-octene (22.10%), *trans-*2-octene (20.76%) and 3-octene (3.65%); and the results for the latter catalyst are *cis-*2-octene (31.89%), *trans-*2-octene (31.43%), 3-octene (15.38%) and 1-octene (13.48%). *Cis-*2-octene is the major product of 2-octanol dehydration over both catalysts. But lower percentages of 1-octene and *cis-*2-octene and greater percentages of 3-octene and *trans-*2-octene are obtained on nanoporous γ-alumina prepared using TX-100. This catalyst shows excessive isomerization of 1-octenes and *cis-*2-octenes to 3-octenes and *trans-*2-octene, respectively.

Fig. 7 displays the products distribution vs. reaction time for dehydration reaction of 2-octanol over the synthesized catalysts. A similar behavior is found for both compounds. Based on these results, as the reaction time increases, the percentages of 1-octene and *cis-*2-octane increase and the percentages of 3-octene and

*trans-*2-octane decrease. Due to the higher stability of *trans-*2-octene than *cis-*2-octene and 3-octene than 1-octene, the elimination reactions over both catalysts are under kinetic control.

The conversion and product selectivity (%) for the elimination reaction of 2-octanol over the synthesized catalysts are presented in **Table 3** and compared with some results from the literature for other γ-alumina catalysts [4, 30, 37]. The product selectivity (%) depends on the type of catalyst, catalyst preparation method, catalyst calcination temperature, acidic and basic properties of catalyst, catalyst amount, reaction temperature and flow rate of reaction [4, 30, 31, 37-41].

The best conversion (97.4 %) for elimination reaction of 2-octanol over γ-alumina was reported where 0.5 g catalyst was used at 280 °C (reaction temperature) and flow rate 2.5 mL/h [37]. Other reactions collected in **Table 3** were performed on 0.5-1 g catalyst, under temperatures higher than 220 °C and flow rates 2.5 mL/h or higher. All the referred reactions had low conversions (13-64 %) [4, 30, 37]. The catalytic activity of the synthesized nanoporous γ-alumina compounds in this study are higher than those reported for γ-alumina catalysts in the literature (**Table 3**). It is found that these catalysts convert 90-99 % of 2-octanol to the alkene products at lower temperature (200 °C) and higher flow rate (5 mL/h) where 0.5 g catalyst was used. Therefore, these compounds can be used as new effective catalysts for dehydration of alcohols.
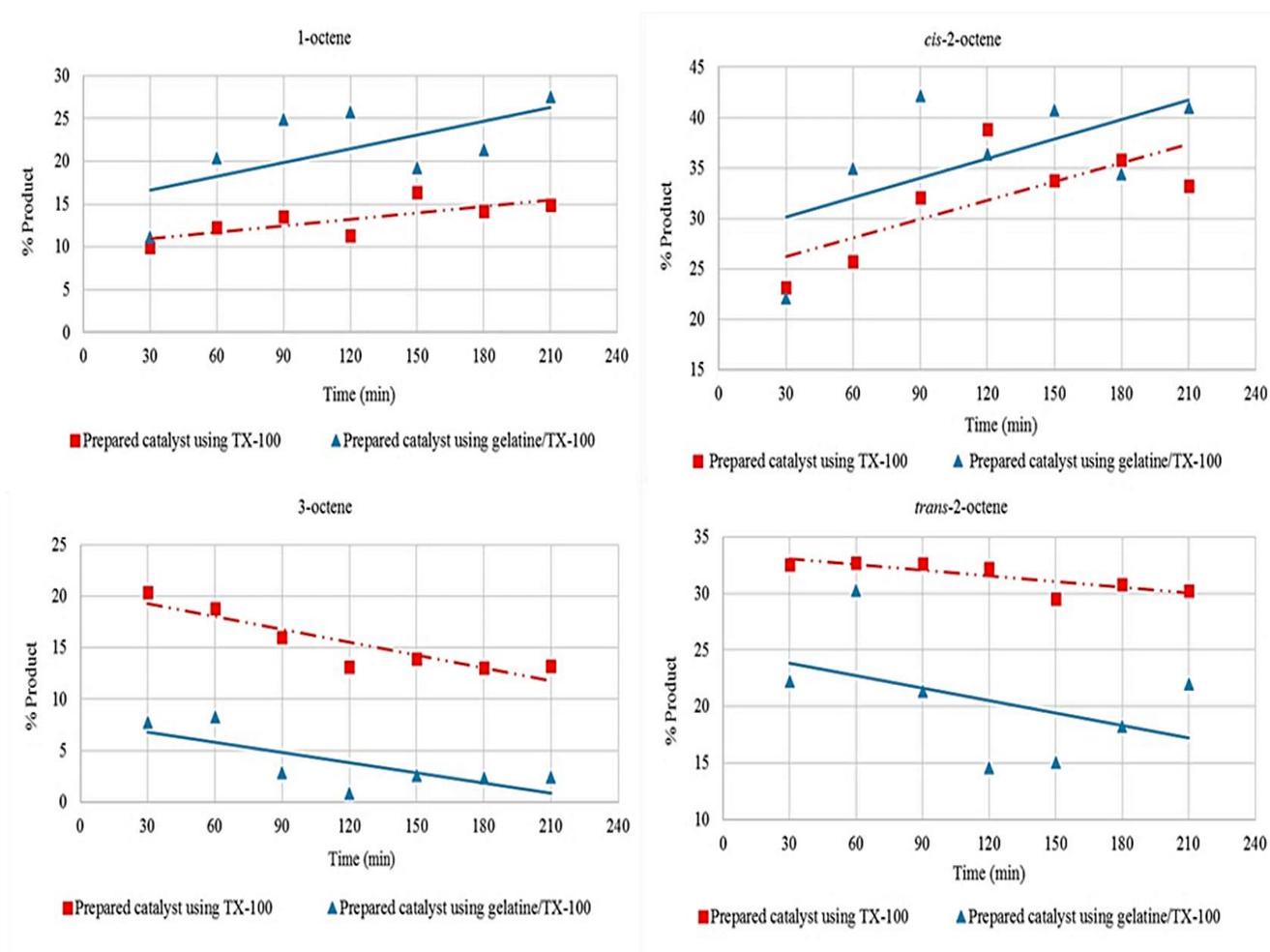
Fig. 7. Products distribution for dehydration reaction of 2-octanol over the synthesized nanoporous γ-alumina catalysts using TX-100 (■) and gelatin/TX-100 (▲).

Table 1. The reaction conversion and yield of the products (%) for the elimination reaction of 2-octanol at 200 °C over the synthesized nanoporous γ-alumina catalyst using TX-100.

Products	Time (min)								Average
	30	60	90	120	150	180	210	240	
1-Octene	9.96	12.29	13.53	11.34	16.32	14.14	14.88	15.36	13.48
3-Octene	20.40	18.80	15.99	13.17	13.90	13.07	13.25	14.50	15.38
Trans-2-octene	32.57	32.74	32.60	32.25	29.55	30.80	30.22	30.72	31.43
Cis-2-octene	23.09	25.70	32.05	38.84	33.76	35.84	33.20	32.65	31.89
2-Octanone	0.30	0.38	2.49	1.49	0.04	0.45	0.38	0.13	0.71
2-Octanol	0.46	0.38	0.16	0.34	0.49	0.56	0.46	0.53	0.42
Byproduct	13.22	9.71	3.18	2.57	5.94	5.14	7.61	6.11	6.68
Conversion**%**	99.54	99.62	99.84	99.66	99.51	99.44	99.54	99.47	99.58

Table 2. The reaction conversion and yield of the products (%) for the elimination reaction of 2-octanol at 200 °C over the synthesized nanoporous γ-alumina catalyst using gelatin/TX-100.

Products	Time (min)								Average
	30	60	90	120	150	180	210	240	
1-Octene	11.07	20.39	24.92	25.77	19.25	21.27	27.49	26.66	22.10
3-Octene	7.67	8.24	2.79	0.82	2.52	2.29	2.42	2.44	3.65
Trans-2-octene	22.17	30.22	21.31	14.57	15.03	18.26	21.97	22.52	20.76
Cis-2-octene	22.03	34.90	42.12	36.34	40.72	34.38	40.94	39.68	36.39
2-Octanone	2.70	0.41	0.22	0.34	0.87	1.02	0.98	0.89	0.93
2-Octanol	5.10	0.67	0.50	15.99	16.55	14.93	0.94	0.49	6.90
Byproduct	29.26	5.17	8.14	6.17	5.06	7.85	5.26	7.32	9.28
Conversion%	94.90	99.33	99.50	84.01	83.45	85.07	99.06	99.51	93.10

The ratio 2-ene/1-ene show selectivity for the formation of 2-alkene. The prepared catalyst using TX-100 have highest selectivity for 2-alkene formation (4.7) among other reported catalysts in **Table 3** (1.1 to 2.6). The 2-ene/1-ene selectivity of this catalyst is 1.8 times greater than that for the catalyst prepared using gelatin/TX-100. Over γ-alumina catalysts from the literature, the selectivity of *cis*-2-octane is 40-50% and the selectivity of *trans* isomer is 10-23% of the total products. The ratio *cis*/*trans* for these compounds is 2.0 to 4.1. No *cis*/*trans* selectivity is observed for γ-alumina catalyst prepared using TX-100 (1.0). The *cis*/*trans* selectivity of this catalyst is lower than that for the catalyst prepared using gelatin/TX-100 by a factor 1.7. The ratio 3-ene/1,2-ene show selectivity for isomerization. This value for γ-alumina catalyst prepared using TX-100 is 0.2 which is 4.3 times greater than γ-alumina catalyst prepared using gelatin/TX-100 and 4.7-200 times greater than other γ-alumina catalysts. So that this catalyst has more potential for isomerization reactions. The behavior of this compound is similar to acidic γ-alumina catalysts, which results in isomerization and 3-octenes creation [31]. The gelatin in the gelatin/TX-100 catalyst reduces the size of catalyst pores which causes the decrease of isomerization and increase of 1-ene formation.

4. Conclusions

The nanoporous γ-alumina catalysts were prepared by sol-gel method using hydrolysis of aluminum isopropoxide in the presence of TX-100 or gelatin/TX-100 mixture. The advantage of this method is the synthesis of γ-alumina with high surface area, large pore volume and nanometer-sized pores. The morphology of catalysts was analyzed by XRD, FT-IR and BET-BJH measurements. The porous nature of catalysts was studied by TEM and nitrogen adsorption-desorption isotherms. Both catalysts display a similar XRD pattern attributing to alumina γ-phase. The nanoporous γ-

alumina prepared using TX-100 had larger surface Parea, crystallite sizes, pore volume and average pore diameter than the nanoporous catalyst prepared using gelatin/TX-100. The catalytic activity of these compounds for dehydration of 2-octanol was higher than those reported for γ-alumina catalysts in the literature. The high conversion for elimination reaction of 2-octanol over γ-alumina was reported previously at high temperatures as 280 °C. While the highest conversion at lower temperature (200 °C) was reported in this study. *Cis*-2-octene is the major product of 2-octanol dehydration over both catalysts. The lower percentages of 1-octene -and cis-2-octene and greater percentages of 3-octene and trans-2-octene were observed on nanoporous γ-alumina prepared using TX-100. The prepared catalyst using TX-100 had high selectivity for 2-alkene formation. This catalyst showed excessive isomerization of 1-octenes and cis-2-octenes to 3-octenes and trans-2-octene, respectively. The gelatin in the gelatin/TX-100 catalyst reduces the size of catalyst pores which causes to decrease of isomerization and increase of 1-ene formation.

Author contributions:

Soheyl Alidoust: Formal analysis, Investigation, Data Curation, Visualization.

Mehdi Zamani: Conceptualization, Methodology, Validation, Formal analysis, Resources, Data Curation, Writing - Original Draft, Writing - Review & Editing, Visualization, Supervision, Project administration, funding acquisition.

Morteza Jabbari: Formal analysis, Resources, Validation.

Table 3. Conversion and product selectivity (%)[a] for elimination reaction of 2-octanol over γ-alumina catalysts at different conditions (i.e. catalyst type, catalyst preparation method and calcination temperature, catalyst amount, reaction temperature and flow rate of reaction).[b-g]

Catalyst type	Catalyst amount (g)	T (°C)	Flow (mL/h)	Conversion (%)	1-octene	trans-2-octene	cis-2-octene	3-Octene	Ratio 2-ene/1-ene	Ratio cis/trans	Ratio 3-ene/1,2-ene
Literature											
γ-Al$_2$O$_3$[b]	0.5	220	2.5	13.2	47	10.3	42.5	0.2	1.1	4.1	0.002
γ-Al$_2$O$_3$[b]	0.5	230	2.5	19.2	44	11.7	44.4	0.1	1.3	3.8	0.001
γ-Al$_2$O$_3$[b]	0.5	240	2.5	30.6	40.9	14	45	0.1	1.4	3.2	0.001
γ-Al$_2$O$_3$[b]	0.5	250	2.5	58.9	38.7	14.8	46.2	0.3	1.6	3.1	0.003
γ-Al$_2$O$_3$[b]	0.5	270	2.5	95.3	35	17.5	47.1	0.4	1.8	2.7	0.004
γ-Al$_2$O$_3$[b]	0.5	280	2.5	97.4	33.2	18.6	47.5	0.7	2.0	2.5	0.007
γ-Al$_2$O$_3$[c]	1.0	280	18.0	47.0	26.0	23.0	46.0	4.0	2.6	2.0	0.042
γ-Al$_2$O$_3$[d]	1.0	280	18.0	64.0	30.0	19.0	48.0	1.2	2.2	2.5	0.012
γ-Al$_2$O$_3$[e]	1.0	280	18.0	46.0	31.0	16.0	50.0	2.3	2.1	3.1	0.023
This work											
γ-Al$_2$O$_3$[f]	0.5	200	5.0	99.6	13.5	31.6	32.0	15.4	4.7	1.0	0.200
γ-Al$_2$O$_3$[g]	0.5	200	5.0	93.1	23.7	22.3	39.1	3.9	2.6	1.7	0.046

[a] Selectivity (%) = (yield/conversion)×100

[b] γ-Alumina (calcined at 400 °C) was obtained from hydrolysis of aluminum nitrate using precipitation method [37]

[c] γ-Alumina (calcined at 600 °C, under atmospheric pressure) was obtained from hydrolysis of aluminum isopropoxide using sol-gel method [4,30]

[d] γ-Alumina (calcined at 600 °C, under 0.01 bar) was obtained from hydrolysis of aluminum isopropoxide using sol-gel method [4]

[e] γ-Alumina (calcined at 600 °C, under 1e^{-6} bar) was obtained from hydrolysis of aluminum isopropoxide using sol-gel method [4]

[f] Nanoporous γ-alumina was obtained from hydrolysis of aluminum isopropoxide using sol-gel method in the presence of TX-100 [This work]

[g] Nanoporous γ-alumina was obtained from hydrolysis of aluminum isopropoxide using sol-gel method in the presence of gelatin/TX-100 [This work]

References

[1] J. W. Anthony, R. A. Bideaux, K. W. Bladh, M. C. Nichols, Handbook of Mineralogy III (Halides, Hydroxides, Oxides), Mineralogical Society of America, Chantilly, VA, US, 1997.

[2] P. S. Santos, H. S. Santos, S. P. Toledo, Standard transition aluminas: Electron microscopy studies, Mater. Res. 3 (2000) 104-114.

[3] W. Smith, R. Chapman, Chemical Process Industries, Vol. 1 inorganic chemicals and allied industries, CBS publishers & distributors Pvt Ltd, India, 2016.

[4] H. A. Dabbagh, K. Taban, M. Zamani, Effects of vacuum and calcination temperature on the structure, texture, reactivity, and selectivity of alumina: Experimental and DFT studies, J. Mol. Catal. A: Chem. 326 (2010) 55-68.

[5] R. T. Yang, Adsorbents: Fundamentals and Applications, John Wiley & Sons Inc., New York, 2003.

[6] L. K. Hudson, C. Misra, A. J. Perrotta, K. Wefers, F. S. Williams, Ullmann's Encyclopedia of Industrial Chemistry, Wiley-VCH, Weinheim, 2005.

[7] Q. Liu, A. Wang, X. Wang, P. Gao, X. Wang, T. Zhang, Synthesis, characterization and catalytic applications of mesoporous -alumina from boehmite sol, Microporous Mesoporous Mater. 111 (2008) 323-333.

[8] M. Zamani, A. Moradi Delfani, M. Jabbari, Scavenging performance and antioxidant activity of γ-alumina nanoparticles towards DPPH free radical: Spectroscopic and DFT-D studies, Spectrochim. Acta A. Mol. Biomol. Spectrosc. 201 (2018) 288-299.

[9] M. Zamani, H. A. Dabbagh, Adsorption behavior of the primary, secondary and tertiary alkyl, allyl and aryl alcohols over nanoscale (1 0 0) surface of γ-alumina, J. Nanoanal. 1 (2014) 21-30.

[10] M. A. Christiansen, G. Mpourmpakis, D. G. Vlachos, Density functional theory-computed mechanisms of

ethylene and diethyl ether formation from ethanol on γ-Al$_2$O$_3$ (100), ACS Catal. 3 (2013) 1965-1975.

[11] Z. Fang, Y. Wang, D. A. Dixon, Computational study of ethanol conversion on Al$_8$O$_{12}$ as a Model for γ-Al$_2$O$_3$, J. Phys. Chem. C 119 (2015) 23413-23421.

[12] K. Larmier, C. Chizallet, N. Cadran, S. Maury, J. Abboud, A. F. Lamic-Humblot, ́E. Marceau, H. Lauron-Pernot, Mechanistic investigation of isopropanol conversion on alumina catalysts: Location of active sites for alkene/ether production, ACS Catal. 5 (2015) 4423-4437.

[13] Z. Zuo, P. Han, J. Hu, W. Huang, Effect of surface hydroxyls on DME and methanol adsorption over γ-Al$_2$O$_3$ (hkl) surfaces and solvent effects: A density functional theory study, J. Mol. Model. 18 (2012) 5107-5111.

[14] Z. Zuo, W. Huang, P. Han, Z. Gao, Z. Li, Theoretical studies on the reaction mechanisms of AlOOH- and γ-Al2O3-catalysed methanol dehydration in the gas and liquid phases, Appl. Catal. A Gen. 408 (2011) 130-136.

[15] H. A. Dabbagh, M. Zamani, B. H. Davis, Nanoscale surface study and reactions mechanism of 2-butanol over the γ-alumina (1 0 0) surface and nanochannel: A DFT study, J. Mol. Catal. A: Chem. 333 (2010) 54-68.

[16] B. Chen, J. Lin, X. Chen, Y. Zheng, H. Zhang, F. Huang, Y. Xiao, Y. Zheng, Controllable synthesis of mesoporous alumina as support for palladium catalysts and reconstruction of active sites during methane combustion, Int. J. Hydrogen Energy 45 (2020) 15142-15156.

[17] X. Song, Y. Song, J. Wang, Q. Liu, Z. Duan, Insights into the pore-forming effect of polyvinyl butyral (PVB) as the polymer template to synthesize mesoporous alumina nanofibers via electrospinning, Ceram. Int. 46 (2020) 9952-9956.

[18] C. Hu, Y. Liu, Q. Cao, L. Bian, Synthesis, characterization, and application of mesoporous alumina prepared from pseudo-boehmite as precursor, Chem. Phys. Lett. 742 (2020) 137130.

[19] R. Ambade, R. Chakravarty, J. Bahadur, B. Ganjave, D. Sen, S. Chakraborty, A. Dash, Mechanochemically synthesized mesoporous alumina: An advanced sorbent for post-processing concentration of 131I for cancer therapy, J. Chromatogr. A 1612 (2020) 460614.

[20] R. Chakravarty, J. Bahadur, S. Lohar, H. D. Sarma, D. Sen, R. Mishra, S. Chakraborty, A. Dash, Solid state synthesis of mesoporous alumina: A viable strategy for preparation of an advanced nanosorbent for 99Mo/99mTc generator technology, Micropor. Mesopor. Mat. 287 (2019) 271-279.

[21] M. Derakhshani, A. Hashamzadeh, M. M. Amini, Novel synthesis of mesoporous crystalline γ-alumina by replication of MOF-5-derived nanoporous carbon template, Ceram. Int. 44 (2018) 17102-17106.

[22] D. Liu, H. Zhu, J. Zhao, L. Pan, P. Dai, X. Gu, L. Li, Y. Liu, X. Zhao, Synthesis of mesoporous γ-Al$_2$O$_3$ with spongy structure: In-situ conversion of metal-organic frameworks and improved performance as catalyst support in hydrodesulfurization, Materials 11 (2018) 1067.

[23] G. Mohammadnezhad, O. Akintola, W. Plass, F. H. Schacher, F. Steiniger, M. Westermann, Facile synthesis of highly thermally stable nanoporous γ-aluminas from aluminum alkoxide precursors, RSC Adv. 5 (2015) 49493-49499.

[24] D. Berger, G. A. Traistaru, C. Matei, Influence of different templates on the morphology of mesoporous aluminas, Cent. Eur. J. Chem. 10 (2012) 1688-1695.

[25] S. Chauhan, J. Jyoti, G. Kumar, Non-ionic surfactant interactions in aqueous gelatin solution: A physico-chemical investigation, J. Mol. Liq. 159 (2011) 196-200.

[26] H. Huang, L. Wang, Y. Cai, C. Zhou, Y. Yuan, X. Zhang, H. Wan, G. Guan, Facile fabrication of urchin-like hollow boehmite and alumina microspheres with a hierarchical structure via Triton X-100 assisted hydrothermal synthesis, Cryst. Eng. Comm. 17 (2015) 1318-1325.

[27] K.B. Djagnya, Z. Wang, S. Xu, Gelatin: A valuable protein for food and pharmaceutical industries, Crit. Rev. Food Sci. Nutr. 41 (2010) 481-492.

[28] A. S. K. de Oliveira, A. P. F. Paulista, A. E. V. de Alencar, T. P. Braga, Gelatin template synthesis of aluminum oxide and/or silicon oxide containing micro/mesopores using the proteic sol-gel method, J. Nanomater. (2017) 2504796.

[29] M. Sobhani, H. Tavakoli, M.D. Chermahini, M. Kazazi, Preparation of macro-mesoporous γ-alumina via biology gelatin assisted aqueous sol-gel process, Ceram. Int. 45 (2019) 1385-1391.

[30] H. A. Dabbagh, M. Zamani, Catalytic conversion of alcohols over alumina–zirconia mixed oxides: Reactivity and selectivity, Appl. Catal. A: General 404 (2011) 141-148.

[31] H. A. Dabbagh, M. Naderi, M. Zamani, Effect of NaNO$_2$, HNO$_3$ and H$_2$SO$_4$ on the structure and reactivity of gamma-alumina, Iran. J. Catal. 10 (2020) 47-55.

[32] J. M. Saniger, Al-O infrared vibrational frequencies of γ-alumina, Mater. Lett. 22 (1995) 109-113.

[33] V. Gonzalez-Pena, I. Dıaz, C. Marquez-Alvarez, E. Sastre, J. Perez-Pariente, Thermally stable mesoporous alumina synthesized with non-ionic surfactants in the presence of amines, Microporous Mesoporous Mater. 44-45 (2001) 203-210.

[34] S. A. Bagshaw, T. J. Pinnavaia, Mesoporous alumina molecular sieves, Angew. Chem. Int. Ed. Engl. 35 (1996) 1102-1105.

[35] K. S.W. Sing, D. H. Everett, R. A. W. Haul, L. Moscou, R. A. Pierotti, J. Roquerol, T. Siemieniewska, Reporting physisorption data for gas/solid systems with special reference to the determination of surface area and porosity, Pure Appl. Chem. 57 (1985) 603-619.

[36] K. S. W. Sing, R. T. Williams, Physisorption hysteresis loops and the characterization of nanoporous materials, Adsorpt. Sci. Technol. 22 (2004) 773-782.

[37] S. Chokkaram, R. Srinivasan, D. R. Milburn, B. H. Davis, Conversion of 2-octanol over nickel-alumina, cobalt-alumina, and alumina catalysts, J. Mol. Catal. A: Chem. 121 (1997) 157-169.

[38] B. H. Davis, Influence of pretreatment of alumina on the dehydrogenation: Dehydration selectivity for 2-octanol, J. Catal. 26 (1972) 348-351.

[39] B. H. Davis, Olefin selectivity for the dehydration of 2-octanol by alumina and thoria, J. Org. Chem. 37 (1972) 1240-1244.

[40] H. A. Dabbagh, J. Mohammad Salehi, New transition-state models and kinetics of elimination reactions of tertiary alcohols over aluminum oxide, J. Org. Chem. 63 (1998) 7619-7627.

[41] M. Zamani, H. A. Dabbagh, Surface modification of γ-alumina by $NaNO_2$, $NaNO_3$, HNO_2, HNO_3 and H_2SO_4: A DFT-D approach, Iran. J. Catal. 6 (2016) 345-353.